Development of Parameter Sensitivity Plot and Application to Modeling of Lithium-ion Secondary Batteries

パラメータ感度プロットの開発とリチウムイオン二次電池のモデリングへの応用

Ichiro MARUTA
丸田 一郎

In this paper, we propose the normalized parameter sensitivity plot as a new tool for analyzing the difficulty of parameter estimation in modeling. The plot visualizes the contribution of the identification inputs to the parameter estimation accuracy and the relative relationship between the estimation accuracy of multiple parameters in the frequency domain. This relative relationship sets a limit on practical estimation accuracy, and the plot is useful for evaluating this limit. As an application example, a model of a rechargeable battery for an electric vehicle is analyzed, and it is shown that the proposed approach can obtain information useful in the selection of model structure and planning of identification experiments.

本稿では，モデリングにおけるパラメータ推定の困難さを解析するための新しいツールとして，正規化パラメータ感度プロットを提案する．このプロットは同定入力のパラメータ推定精度への寄与と，複数のパラメータの推定精度の相対的な関係を周波数領域において可視化する．この相対的な関係によって実際的な推定精度の限界が定まり，その推定精度限界の評価にプロットが有用であることが示される．また，提案法の活用例として電気自動車用の充電式電池のモデルを解析し，モデル構造の選択やパラメータ推定に必要な実験の計画において有用な情報が得られることを示す．

Introduction

In the next generation society, it is necessary to control large-scale network systems such as smart grids and complex systems such as human behavior. For designing control systems, model construction is indispensable, and the conventional approach is to prepare a model with the same structure as the system and estimate the parameters included in the model from the data. However, it is unrealistic to build a model with an equivalent structure for complex / large-scale systems and estimate the parameters with the required accuracy. Thus, it is necessary to simplify the model structure.

From this aspect, it is important to know the degree of the difficulty in estimating parameters for a given model structure, and the Cramér-Rao bound is known to be a powerful tool especially for linear time-invariant models.[1] By using the bound, we can predict how accurate the estimate can be once we know the amount of noise. The results also can be interpreted in the frequency domain.[2] However, in practical problems, many uncertain factors, such as the error caused by the inconsistency between the model structure and the target system, should be handled as noise. Thus, it is not straightforward to estimate the difficulty based on the Cramér-Rao bound, which depends on the noise spectrum.

For this background, we introduce a new practically useful tool for discussing the degree of the difficulty in estimating parameters in linear time-invariant continuous-time models. The newly introduced tool is the normalized parameter sensitivity plot. In the plot, spectral characteristics of the normalized parameter sensitivities of a continuous-time transfer function model G with a set of parameter $\boldsymbol{\theta} \triangleq [\theta_1,\theta_2,...,\theta_{n_\theta}]^{\mathrm{T}}$, that is,

$$\theta_1 \frac{\partial G}{\partial \theta_1}, \theta_2 \frac{\partial G}{\partial \theta_2},..., \theta_n \frac{\partial G}{\partial \theta_{n_\theta}}$$

are plotted in one figure. For example, the normalized parameter sensitivity plot for the mass-spring-damper system whose structure is shown in Figure 1a and with the parameter

$$\boldsymbol{\theta} \triangleq [m_1, k_1, d_1, m_2, k_2, d_2, m_3, k_3, d_3]^{\mathrm{T}} \quad \cdots\cdots\cdots\cdots \quad (1)$$
$$= [100, 100, 100, 10, 10, 10, 1, 1, 1]^{\mathrm{T}}$$

is shown in Figure 1b. In this paper, it is shown that a practically important limitation on the estimation accuracy, which does not depend on noise spectrum, is derived by focusing on the relative positions of the plots.

This paper is based on the authors' previous work[3] and organized as follows. First, we review the relationship between the parameter sensitivity and the estimation accuracy in Section "**Parameter sensitivity and difficulty in estimating parameter**". In Section "**Normalized parameter sensitivity plot**", the usage of the normalized sensitivity plot is proposed, and its theoretical background is described. In Section "**Application to battery system**", a lithium-ion rechargeable battery model is analyzed by the proposed approach to show how the normalized parameter sensitivity plot is used in practical problems. Finally, Section "**Conclusion**" concludes the paper.

In this paper, we denote the differential operator and the Laplace operator with p and s, respectively. For transfer functions G_1 and G_2, their inner product is denoted by

$$\langle G_1, G_2 \rangle \triangleq \frac{1}{2\pi} \int_{-\infty}^{\infty} G_1(j\omega)\overline{G_2(j\omega)}\mathrm{d}\omega,$$

and the norm is defined as

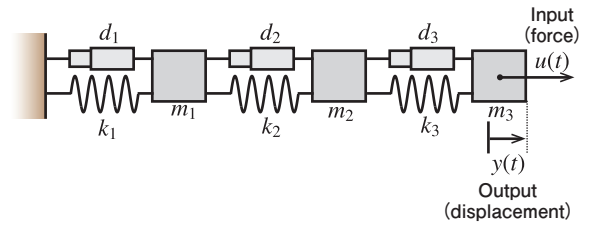

(a) Model

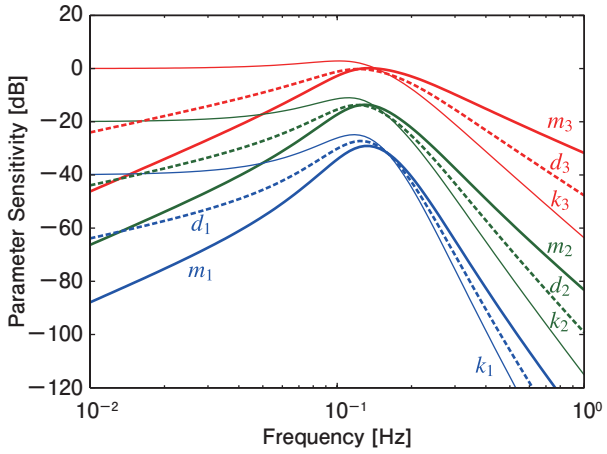

(b) Normalized parameter sensitivity plot

Figure 1 Illustrative example (mass-spring-damper system)

$$\|G_1\| \triangleq \langle G_1, G_2 \rangle^{\frac{1}{2}}$$

For a matrix M, $\|M\|_2$ is the norm defined by the maximum singular value of M. In addition, $\mathrm{cov}(\cdot)$ and $\mathrm{var}(\cdot)$ denote the covariance matrix and the variance, respectively.

Parameter Sensitivity and Difficulty in Estimating Parameters

In this section, the relationship between the normalized parameter sensitivity $\theta_k(\partial G / \partial \theta_k)$ and the estimation accuracy is reviewed.

Problem formulation

First, the setting of the estimation problem, on which the discussion about the estimation accuracy is based, is described. The target system is a single input and single output continuous-time linear time-invariant system, whose input $u(t)$ and output $y(t)$ are related through the differential equation

$$y_0(t) = G(p, \boldsymbol{\theta})u(t)$$

and

$$y(t) = y_0(t) + v(t) \ .$$

Here, $v(t)$ is a zero-mean normally distributed random noise with the power spectral density $\Phi(\omega)$, and $G(p,\boldsymbol{\theta})$ is a rational function of the differential operator p and parametrized by $\theta \triangleq [\theta_1,...,\theta_{n_\theta}]^{\mathrm{T}}$ (the parameter to be estimated). We assume that the parameters $\{\theta_1,...,\theta_{n_\theta}\}$ have ratio scale, that is, each parameter is a quantity for which we can construct a meaningful fraction. Examples of quantities with ratio scale include mass, length, resistance, capacitance and the Kelvin temperature. Celsius temperature is not a ratio scale since it does not have absolute zero and we cannot construct a meaningful fraction of two temperatures. As for the input, $u(t)$ equals 0 when $t < 0$ and is a known square-integrable function. Also, we let $Y_0(s)$ and $U(s)$ be the Laplace transforms of $y_0(t)$ and $u(t)$, respectively.

For this system, we consider the accuracy of the unbiased parameter estimate $\hat{\boldsymbol{\theta}}$ calculated from the system output sampled with time interval h, that is,

$$y \triangleq [y_1,..., y_N]^{\mathrm{T}},$$
$$y_k \triangleq y((k-1)h),$$

where N is the number of available samples.

Since the parameters $\{\theta_1,...,\theta_{n_\theta}\}$ are assumed to have ratio

scale, we focus on the normalized estimate of the parameter

$$\tilde{\boldsymbol{\theta}} \triangleq [\tilde{\theta}_1,\ldots,\tilde{\theta}_{n_\theta}]^{\mathrm{T}} \triangleq \left[\frac{\hat{\theta}_1}{\theta_1},\ldots,\frac{\hat{\theta}_{n_\theta}}{\theta_{n_\theta}}\right]^{\mathrm{T}},$$

to make the comparison between parameters more clear and use $\mathrm{cov}(\tilde{\boldsymbol{\theta}})$ for evaluating the accuracy of the estimate.

Cramér-Rao Bound and Parameter Sensitivity
It is well known that the Cramér-Rao inequality

$$\mathrm{cov}(\tilde{\boldsymbol{\theta}}) \geq I^{-1} \quad \cdots\cdots (2)$$

holds for the unbiased estimate $\tilde{\boldsymbol{\theta}}$, where I is the Fisher information matrix. For the measurement $\boldsymbol{y}$ with sufficiently small sampling interval ($h\to 0$) and long time span ($Nh\to\infty$), (m,n)-element of I asymptotically satisfies

$$I_{mn} = \frac{\theta_m\theta_n}{2\pi h}\int_{-\infty}^{\infty}\frac{1}{\Phi(\omega)}\frac{\partial Y_0(j\omega)}{\partial\theta_m}\overline{\frac{\partial Y_0(j\omega)}{\partial\theta_n}}\,\mathrm{d}\omega$$
$$= \frac{\theta_m\theta_n}{2\pi h}\int_{-\infty}^{\infty}\frac{|U(j\omega)|^2}{\Phi(\omega)}\frac{\partial G(j\omega)}{\partial\theta_m}\overline{\frac{\partial G(j\omega)}{\partial\theta_n}}\,\mathrm{d}\omega \quad \cdots\cdots (3)$$

as shown in.[2] This equation associates the normalized parameter sensitivity θ_m $(\partial G/\partial\theta_m)$ with the estimation accuracy.

Especially, if $v(t)$ is a white noise, Equation 3 can be rewritten as

$$I_{mn} = \frac{\theta_m\theta_n}{2\pi h\sigma^2}\int_{-\infty}^{\infty}|U(j\omega)|^2\frac{\partial G(j\omega)}{\partial\theta_m}\overline{\frac{\partial G(j\omega)}{\partial\theta_n}}\,\mathrm{d}\omega$$
$$= \frac{\theta_m\theta_n}{2\pi h\sigma^2}\left\langle U\frac{\partial G}{\partial\theta_m}, U\frac{\partial G}{\partial\theta_n}\right\rangle,$$

where σ^2 is the variance of the sampled $v(t)$.

Normalized Parameter Sensitivity Plot

Next, we discuss how the normalized parameter sensitivity plot can be utilized for evaluating the difficulty in estimating the parameters based on Equation 2 and Equation 3.

Information from single parameter sensitivity plot

In preparation for stating the main result related to multiple parameter sensitivity plots, the information obtained from a single parameter sensitivity plot is summarized.

For the estimation accuracy of m-th parameter θ_m,

$$\mathrm{var}(\tilde{\theta}_m) \geq (I_{mn})^{-1}$$

holds,[4] and together with (3),

$$\mathrm{var}(\tilde{\theta}_m) \geq \frac{1}{2\pi h}\left(\int_{-\infty}^{\infty}\left|\theta_m\frac{\partial G(j\omega)}{\partial\theta_m}\right|^2\frac{|U(j\omega)|^2}{\Phi(\omega)}\mathrm{d}\omega\right)^{-1} \quad \cdots\cdots (4)$$

is derived. Especially, if $v(t)$ is a white noise, Equation 4 can be written as

$$\mathrm{var}(\tilde{\theta}_m) \geq \frac{\sigma^2}{h}\left\|\theta_m\frac{\partial G}{\partial\theta_m}U\right\|^{-2}.$$

These results are well-known,[1] and Equation 4 shows that the frequency band of the identification input u which is important for estimating θ_m is indicated by the normalized parameter sensitivity function θ_m $(\partial G/\partial\theta_m)$.

For example, the peaks of the normalized parameter sensitivity plots in Figure 1b are concentrated on the resonant frequency of the system and lead to the conclusion that the identification input with such frequency spectrum is effective as expected.

Information from relative parameter sensitivity

In practical problems, model structures cannot be completely consistent with the target systems, and the error stem from the inconsistency is also contained in the measurement error $v(t)$. Since the frequency spectrum of such error strongly depends on the identification input u and is difficult to estimate, the absolute value of the lower bound estimated with Equation 3 is often unreliable.

To deal with the problem, we focus on the relative bound for the estimation variances of the parameters. For the physically meaningful parameters, we often have prior knowledge about the parameter uncertainty to a greater or lesser extent. For example, mechanical friction is normally non-linear phenomenon and it seems impossible to determine friction coefficients with the accuracy better than 10%. Together with such information, the following theorem which gives the relative lower bound for the estimation variance is useful.

Theorem 1: Assume the identification input signal u has spectrum in a band Ω, that is,

$$\omega \notin \Omega \Rightarrow U(j\omega) = 0,$$

and let σ_m^2 be the variance of the efficient estimate of a parameter $\tilde{\theta}_m$. Then, the variance of the estimate of another parameter $\tilde{\theta}_n$ satisfies

$$\mathrm{var}(\tilde{\theta}_m) \geq \left(\inf_{\omega \in \Omega} \left| \frac{\theta_m \dfrac{\partial G(j\omega)}{\partial \theta_m}}{\theta_n \dfrac{\partial G(j\omega)}{\partial \theta_{mn}}} \right| \right)^2 \sigma^2{}_m.$$

Proof: See [3].

Theorem 1 states that there is a limitation on the estimation accuracy, which does not depend on the noise spectrum and the detail of the identification input. The coefficient which characterizes the limitation

$$\inf_{\omega \in \Omega} \left| \frac{\theta_m \dfrac{\partial G(j\omega)}{\partial \theta_m}}{\theta_n \dfrac{\partial G(j\omega)}{\partial \theta_{mn}}} \right|$$

corresponds to the distance in the normalized parameter sensitivity plot. Since Theorem 1 holds regardless of the noise spectrum, it gives information about the estimation variance even under the existence of noise with unknown spectrum.

Remark 1: If the normalized parameter sensitivity plot for θ_n dips below the one for θ_m by x [dB], the standard deviation of $\tilde{\theta}_n$ is at least x [dB] larger than the one achievable for $\tilde{\theta}_m$.

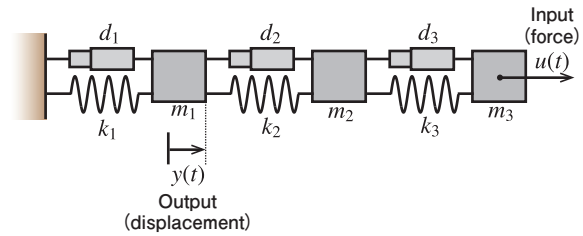

(a) Model

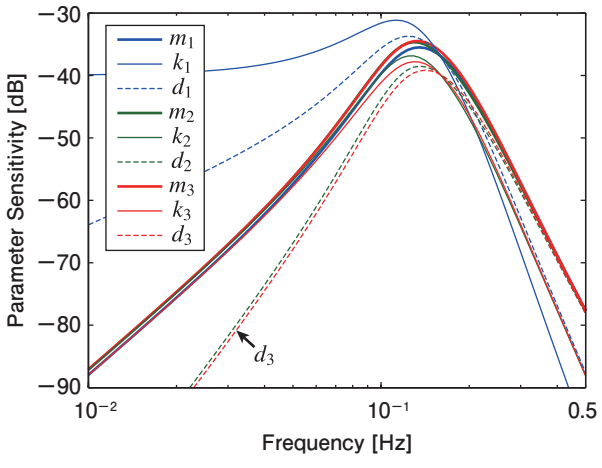

(b) Normalized parameter sensitivity plot

Figure 2 Parameter sensitivity plot for improved mass-spring-damper system (displacement of m_1 is measured instead of m_3)

For example, if d_3 in Figure 1 has 10% uncertainty, the standard deviation of the estimate for d_1 is larger than 100% since the normalized sensitivity for d_1 is smaller than that for d_3 by more than 20 dB, and the estimation of d_1 is found to be impossible in practice. For this example, distances between the sensitivity plots can be made smaller by measuring the displacement of m_1 instead of m_3 (see Figure 2), and the difficulty in estimating the parameters can be reduced. Although the improvement made by changing the measured variable is intuitively acceptable, the absolute value of the sensitivity is not improved from Figure 1 to Figure 2, and this improvement is not explained easily without evaluating the relative relationship between the parameter sensitivity.

Application to Battery System

Next, a model of a lithium-ion rechargeable battery for electric vehicles is analyzed by the proposed approach to illustrate the effectiveness of the approach in realistic situations. Indeed, the estimation of the detailed status of the battery is the key for improving the energy efficiency while preserving safety (see [5] and references therein), and it is important to know the degree of the difficulty in estimating the parameters related to the battery status.

In this paper, we consider the linear battery model shown in Figure 3. In the figure, R_0 represents the DC resistance of the electrolyte, C represents the linearized relationship between the state of charge (SOC) and the open circuit voltage (OCV), and Z_w represents the Warburg impedance which models the ion diffusion process.[6] The relationship between the input current (= $u(t)$) and the output voltage (= $y(t)$) of the battery model can be described by the transfer function

$$G_d(s) = \frac{k}{\mathrm{FCC}_0 \cdot \mathrm{SOH}} \frac{1}{s} + R_0 + \frac{R_d}{\sqrt{\tau_d s}} \tanh \sqrt{\tau_d s}\,. \quad \cdots\cdots (5)$$

In Equation 5, the first term corresponds to C in the figure; k is the proportionality coefficient for the linearly approximated relationship between the SOC and the

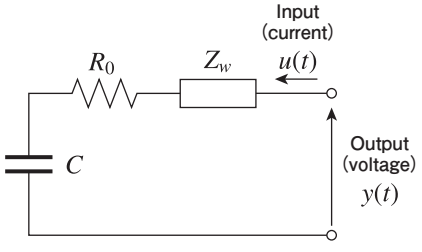

Figure 3 Linear circuit model for Lithium-ion battery

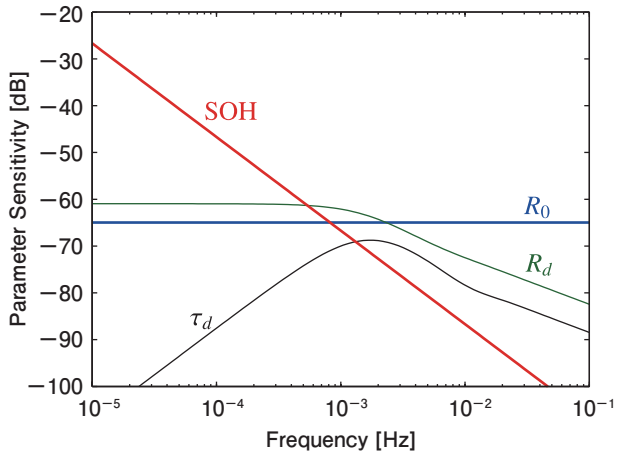

Figure 4 Normalized parameter sensitivity plot for battery model with Warburg impedance diffusion process model (G_d)

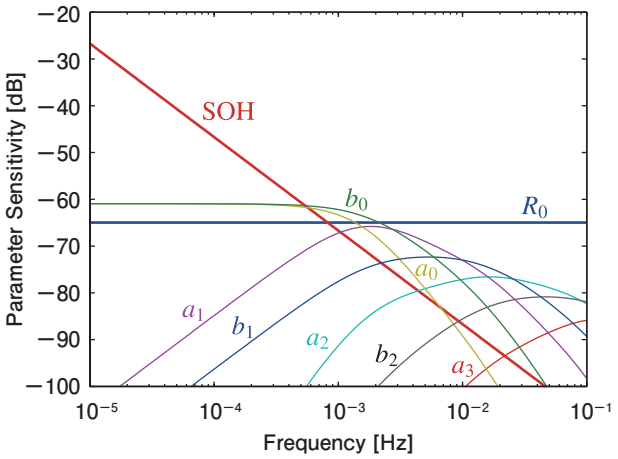

Figure 5 Normalized parameter sensitivity plot for battery model with generic transfer function diffusion process model (G_r)

OCV; FCC_0 is the full charge capacity for the brand-new battery; and SOH is the state of health parameter which represents the degree of battery deterioration.

For this model, we consider the difficulty in estimating the parameter

$$\boldsymbol{\theta}_d = [R_0,\ R_d,\ \tau_d,\ \mathrm{SOH}]^{\mathrm{T}}$$

based on the proposed approach. Since rough value of the parameters are required for the analysis, we use R_0 = 0.565 mΩ, R_d = 0.896 mΩ, τ_d = 224 s, SOH = 91%, and $FCC_0 = 2.36\times10^5$ C, which are estimated from the experiment in the literature.[7]

Figure 4 shows the normalized parameter sensitivity plot for the model. From the figure, we can conclude that:

- For reliably estimating SOH, or the degree of battery deterioration, data with a time span longer than 2000 s are desired since the parameter sensitivity for SOH is relatively smaller than that for the other parameters for the frequency higher than 10^{-3} Hz.
- For estimating SOH in a shorter time, the uncertainties of R_d, R_0 and τ_d are the most important bottle necks in this order since the normalized sensitivities for these parameters surpass that for SOH in this order when increasing the frequency.
- The estimation of τ_d is relatively more difficult because the normalized parameter sensitivity for τ_d never come on the top. And, the identification input around 0.002 Hz is most effective.

This information is of great value in devising strategies for estimating the battery statuses, such as, the level of deterioration, and is consistent with the empirical knowledge of the battery. Note that the batteries for electric vehicles are used on a time scale larger than hours, and the time scale of the information obtained by analyzing the plot is reasonable.

In addition, we attempt to evaluate another model structure. In Equation 5, we adopted the Warburg impedance model for the ion diffusion process.
However, it is also possible to adopt generic rational transfer function model

$$G_r(s) = \frac{k}{\mathrm{FCC}_0 \cdot \mathrm{SOH}}\frac{1}{s} + R_0 + \frac{b_2 s^2 + b_1 s + b_0}{a_3 s^3 + a_2 s^2 + a_1 s + a_0} \quad \cdots\cdots (6)$$

for the process. Here, the order of the transfer function model is set three because the number is enough for approximating the Warburg impedance model for practical I/O data.[7] Since this model have larger number of parameters than Equation 5, it might be possible to provide models with greater accuracy.

For this model, the normalized parameter sensitivity plot for the parameter

$$\boldsymbol{\theta}_r = [R_0,\ SOH,\ a_0,\ a_1,\ a_2,\ a_3,\ b_0,\ b_1,\ b_2]^{\mathrm{T}}$$

is shown in Figure 5. In the figure, the plots for b_2 and a_3 dip below the one for R_0 by nearly 20 dB. The uncertainty of R_0 is empirically not smaller than 10%, one cause of which is thought to be unmodeled dependency on the temperature, we can conclude that it is impossible to obtain dependable estimates of b_2 and a_3.

On the other hand, the largest distance among the normalized parameter sensitivities is around 5 dB for Figure 4, and there is no major problem predicted from Theorem 1. Therefore, we can conclude that the model Equation 5 is more promising.

As shown in this example, the normalized parameter sensitivity plot can be utilized for devising strategies for estimating parameters and selecting models with appropriate

complexity.

Conclusion

In this paper, the analysis based on the normalized parameter sensitivity plot is introduced for evaluating the degree of the difficulty in estimating model parameters. From the plot, the limitation on the estimation accuracy, which stems from the relative relationship between the model sensitivities for the parameters, is easily obtained. The theoretical background of this limitation is shown, and an example with a rechargeable battery system is shown to illustrate how the proposed approach provides valuable information in practical problems.

The proposed approach can be expected to be a useful tool for dealing with large-scale complex systems in the next generation society. Part of its usefulness is shown in the example of the rechargeable battery, which plays a crucial role in the next generation society.

References

[1] L. Ljung, System Identification: Theory for the User, Second ed., Prentice-Hall, 1999.

[2] A. Zeira and A. Nehorai, "Frequency domain Cramer-Rao bound for Gaussian processes," *IEEE Transactions on Acoustics, Speech and Signal Processing*, vol. 38, pp. 1063-1066, 1990.

[3] I. Maruta, A. Baba and S. Adachi, "Analysis of difficulty in estimating physically-meaningful model parameters based on normalized parameter sensitivity plot," in *the 54th IEEE Conference on Decision and Control (CDC)*, 2015.

[4] B. Z. Bobrovsky, E. Mayer-Wolf and M. Zakai, "Some Classes of Global Cramér-Rao Bounds," *The Annals of Statistics*, vol. 15, pp. 1421-1438, 1987.

[5] L. Lu, X. Han, J. Li, J. Hua and M. Ouyang, "A review on the key issues for lithium-ion battery management in electric vehicles," *Journal of Power Sources*, vol. 226, pp. 272-288, 2013.

[6] D. Di Domenico, E. Prada and Y. Creff, "An Adaptive Strategy for Li-ion Battery SOC Estimation," in *Proceedings of the 18th IFAC World Congress*, Milano, 2011.

[7] T. Kawaguchi, I. Maruta, A. Baba and S. Adachi, "Continuous-time System Identification of Rechargeable Battery in Electric Vehicles in Consideration of Diffusion Phenomena," *Transactions of the Society of Instrument and Control Engineers*, vol. 49, pp. 670-677, 2013.

Ichiro MARUTA
丸田 一郎
Associate Professor
Department of Aeronautics and Astronautics,
Graduate School of Engineering, Kyoto University
Doctor of Informatics